N90-13415

AUTONOMOUS SPACECRAFT ATTITUDE CONTROL
USING MAGNETIC TORQUING ONLY

Keith L. Musser
Ward L. Ebert
The Johns Hopkins University
Applied Physics Laboratory
Laurel, Maryland 20707

ABSTRACT

Magnetic torquing of spacecraft has been an important mechanism for attitude control since the earliest satellites were launched. Typically a magnetic control system has been used for precession/nutation damping for gravity-gradient stabilized satellites, momentum dumping for systems equipped with reaction wheels, or momentum-axis pointing for spinning and momentum-biased spacecraft. Although within the small satellite community there has always been interest in inexpensive, light-weight, and low-power attitude control systems, completely magnetic control systems have not been used for autonomous three-axis stabilized spacecraft due to the large computational requirements involved. As increasingly more powerful microprocessors have become available, this has become less of an impediment. These facts have motivated consideration of the all-magnetic attitude control system presented here.

The problem of controlling spacecraft attitude using only magnetic torquing is cast into the form of the Linear Quadratic Regulator (LQR), resulting in a linear feedback control law. Since the geomagnetic field along a satellite trajectory is not constant, the system equations are time varying. As a result the optimal feedback gains are time-varying. Orbit geometry is exploited to treat feedback gains as a function of position rather than time, making feasible the onboard solution of the optimal control problem. In simulations performed to date, the control laws have shown themselves to be fairly robust and a good candidate for an onboard attitude control system.

INTRODUCTION

Magnetic torquing has been used for spacecraft attitude control since the launch of the earliest satellites. There are many operational spacecraft which use magnetics for precession/nutation damping, momentum dumping, and large angle maneuvers [1-4]. Also, there are existing three-axis control systems which use magnetic torquing to maintain spin axis orientation of a pitch reaction wheel [5]. Use of magnetics has recently been suggested for libration damping and arbitrary yaw angle control of a gravity gradient stabilized satellite [7].

Complete three-axis attitude control has not been used because of the large computational requirements involved. As increasingly more powerful microprocessors have become available, computation has become less of an impediment. This has motivated consideration of the all-magnetic attitude control system presented here.

We consider a rigid spacecraft without a gravity gradient boom. For the present discussion, we assume a perfect knowledge of the spacecraft attitude is available. Finally, we assume the spacecraft is in a near circular orbit and has a nadir pointing nominal attitude.

The geomagnetic field, while essentially constant in an earth-fixed reference frame, is time-varying in the nominal body reference frame. This introduces a time-varying element into the linearized system of equations. Because the magnetic torque vector is constrained to always lie perpendicular to the local geomagnetic field vector, the system appears uncontrollable if fixed at any instant in time. (When considered over time, it is completely controllable.) This does, however, limit the achievable closed loop transient reaction speed to the order of magnitude of the magnetic field time variation. For a nadir pointing satellite in a polar orbit, this is about two cycles per orbit. The reaction speed should decrease with decreasing orbit inclination because the geomagnetic field variation decreases in magnitude.

FORMULATION OF THE EQUATIONS OF MOTION

Nomenclature

LQR	Linear Quadratic Regulator
P, R, Y	Pitch, Roll, Yaw (2-1-3 Euler angles)
ω_o	Mean angular rate of the local vertical reference frame.
$R_i(\theta)$	Rotation matrix for an angle θ about the i-axis.
$C_{B \leftarrow S}$	Rotation matrix from inertial (space) to actual body coordinates.
$C_{N \leftarrow S}$	Rotation matrix from inertial (space) to nominal body coordinates.
$C_{B \leftarrow N}$	Rotation matrix from nominal body to actual body coordinates.
ω_B	Angular velocity of spacecraft with respect to inertial frame, represented in the body frame.
τ_B	Total external torque acting on spacecraft body, in body frame.

$T_{dist,B}$	External disturbance torque, excluding gravity gradient torque, represented in the body frame.
$T_{con,B}$	Control torque acting on spacecraft body, represented in body frame.
R_s	Magnitude of spacecraft position vector in Earth centered coordinates.
$\hat{R}_B$	Unit vector from center of Earth to spacecraft, represented in the body frame.
J	Spacecraft inertia tensor, represented in the body frame.
$J_i \{J_1, J_2, J_3\}$	i^{th} diagonal element of inertia matrix J.
$d_B(t)$	Control dipole moment of spacecraft, represented in the body frame.
H_B	Local geomagnetic field intensity, represented in the body frame.
$H_N(t)$	Local geomagnetic field intensity, represented in the nominal body frame.
μ	Geocentric gravitational constant, $GM_E = \mu = 3.986 \times 10^{14}$ m^3/s^2.
$h_i(t) \{h_1(t), h_2(t), h_3(t)\}$	i^{th} component of $H_N(t)$.
$d_i(t) \{d_1(t), d_2(t), d_3(t)\}$	i^{th} component of $d_B(t)$.
$x(t)$	State vector $[R, P, Y, \dot{R}, \dot{P}, \dot{Y}]^T$.
F	System matrix of linearized equations.
$G(t)$	Input coupling matrix of linearized equations.
$J(d_B(t))$	Quadratic cost functional.
S_f	Final time state cost matrix.
A	State cost weighting matrix.
B	Control cost weighting matrix.
$S(t)$	Solution of the matrix Riccati equation.
$K(t)$	Feedback gain matrix, parameterized by time.
$K(\beta, \lambda)$	Feedback gain matrix, parameterized by (β, λ).
a	Orbit semi-major axis
e	Orbit eccentricity.
i	Orbit inclination.

Ω	Argument of the ascending node.
ω	Argument of perigee.
ω_E	Angular rate of the Earth $\approx 2\pi$ radians/24 hours.
λ	Earth fixed longitude of the ascending node.
β	Argument of latitude (defined in Figure 4).

FORMULATION OF THE EQUATIONS OF MOTION

For the problem at hand, we have considered the rigid-body equations of motion of a nadir-pointing spacecraft in a circular orbit. Referring to Figure 1, where (S) subscripts indicate inertial frame, (N) indicates nominal body frame, and (B) indicates actual body frame, we can represent attitude using 2-1-3 Euler angles as

$$C_{B \leftarrow S} = R_3(Y)\, R_1(R)\, R_2(\omega_o t + P) \tag{1}$$

$$C_{B \leftarrow S} = R_3(Y)\, R_1(R)\, R_2(P)\, R_2(\omega_o t) \tag{2}$$

where $R_i(\theta)$ is a rotation about axis i through angle θ. Since the desired trajectory has Y, R, and P all zero, we can define an intermediate "nominal" attitude (to be used later) as

$$C_{N \leftarrow S} = R_2(\omega_o t)\ , \tag{3}$$

which gives

$$C_{B \leftarrow N} = R_3(Y)\, R_1(R)\, R_2(P)\ . \tag{4}$$

The angular velocity of the body frame with respect to the inertial frame can be expressed as

$$\underline{\omega}_B = \dot{Y}\begin{bmatrix} 0 \\ 0 \\ 1 \end{bmatrix} + R_3(Y)\,\dot{R}\begin{bmatrix} 1 \\ 0 \\ 0 \end{bmatrix} + R_3(Y)\, R_1(R)\, (\omega_o + \dot{P})\begin{bmatrix} 0 \\ 1 \\ 0 \end{bmatrix}\ . \tag{5}$$

To first order in angles and rates this is

$$\underline{\omega}_B = \begin{bmatrix} \dot{R} + \omega_o Y \\ \omega_o + \dot{P} \\ \dot{Y} - \omega_o R \end{bmatrix}\ . \tag{6}$$

To obtain the first-order approximations to Euler's equations we write

$$\underline{\tau}_B = \frac{d}{dt}(J\,\underline{\omega}_B) + \underline{\omega}_B \times J\,\underline{\omega}_B\ , \tag{7}$$

which, assuming a diagonal inertia matrix, gives

$$\mathbf{\underline{\tau}_B} \approx \begin{bmatrix} J_1 \ddot{R} + \omega_o(J_1 + J_3 - J_2) \dot{Y} + \omega_o^2(J_2 - J_3) R \\ J_2 \ddot{P} \\ J_3 \ddot{Y} - \omega_o(J_1 + J_3 - J_2) \dot{R} + \omega_o^2(J_2 - J_1) Y \end{bmatrix} \qquad (8)$$

The applied torque $\underline{\tau}_B$ consists of the gravity gradient, control, and disturbance torques, and can be represented as

$$\underline{\tau}_B = \underline{\tau}_{dist,B} + \underline{\tau}_{con,B} + \frac{3\mu}{R_s^3}\left[\widehat{\underline{R}}_B \times (J\,\widehat{\underline{R}}_B)\right] \; , \qquad (9)$$

where R_s is the geocentric radius, and $\widehat{\underline{R}}_B$ is the unit vector from the earth to the spacecraft, represented in the body frame. Since $\widehat{\underline{R}}_B$ corresponds to the z-axis in the nominal reference frame, we can use the first-order approximation

$$\widehat{\underline{R}}_B = \begin{bmatrix} -P \\ R \\ 1 \end{bmatrix} \; , \qquad (10)$$

giving

$$\underline{\tau}_B = \underline{\tau}_{dist,B} + \underline{\tau}_{con,B} - \frac{3\mu}{R_s^3}\begin{bmatrix} (J_2 - J_3) R \\ (J_1 - J_3) P \\ 0 \end{bmatrix} \; . \qquad (11)$$

Finally, we examine the control torque $\underline{\tau}_{con,B}$. This torque is obtained from the commanded dipole $\underline{d}_B(t)$ as

$$\underline{\tau}_{con,B} = \underline{d}_B(t) \times \underline{H}_B \qquad (12)$$

where $\underline{H}_B$ is the ambient field intensity represented in the body frame. We also have

$$\underline{H}_B = C_{B \leftarrow N}\, \underline{H}_N(t) \approx \underline{H}_N(t) \qquad (13)$$

where the explicit time dependence applied to $\underline{H}_N(t)$ emphasizes that its value is attitude independent. We would like to replace $\underline{H}_B$ in equation (12) with $\underline{H}_N(t)$. This is valid as a first-order approximation because we will later be assigning a control law for $\underline{d}_B(t)$ which is linear in angles and rates.

Combining equations (8), (11), and (12) with the approximation (13), we obtain the complete linearized equations of motion as follows:

$$\underline{\dot{x}}(t) = \frac{d}{dt}\begin{bmatrix} R \\ P \\ Y \\ \dot{R} \\ \dot{P} \\ \dot{Y} \end{bmatrix} \begin{bmatrix} 0 & 0 & 0 & 1 & 0 & 0 \\ 0 & 0 & 0 & 0 & 1 & 0 \\ 0 & 0 & 0 & 0 & 0 & 1 \\ F41 & 0 & 0 & 0 & 0 & F46 \\ 0 & F52 & 0 & 0 & 0 & 0 \\ 0 & 0 & F63 & F64 & 0 & 0 \end{bmatrix} \begin{bmatrix} R \\ P \\ Y \\ \dot{R} \\ \dot{P} \\ \dot{Y} \end{bmatrix} +$$

$$
\begin{bmatrix}
0 & 0 & 0 \\
0 & 0 & 0 \\
0 & 0 & 0 \\
0 & G42(t) & G43(t) \\
G51(t) & 0 & G53(t) \\
G61(t) & G62(t) & 0
\end{bmatrix}
\begin{bmatrix}
d_1(t) \\
d_2(t) \\
d_3(t)
\end{bmatrix}
+ \tau_{dist,B}
$$

where

$$F41 = -\frac{J_2-J_3}{J_1}\left(\omega_0^2 + \frac{3\mu}{R_s^3}\right)$$

$$G51(t) = -h_3(t)\, J_2^{-1}$$

$$F52 = -\frac{3\mu}{R_s^3}\left(\frac{J_1-J_3}{J_2}\right)$$

$$G61(t) = h_2(t)\, J_3^{-1}$$

$$F63 = -\omega_0^2\left(\frac{J_2-J_1}{J_3}\right)$$

$$G42(t) = h_3(t)\, J_1^{-1}$$

$$F64 = \omega_0\left(\frac{J_1+J_3-J_2}{J_3}\right)$$

$$G62(t) = -h_1(t)\, J_3^{-1}$$

$$F46 = -\omega_0\left(\frac{J_1+J_3-J_2}{J_1}\right)$$

$$G43(t) = -h_2(t)\, J_1^{-1}$$

$$G53(t) = h_1(t)\, J_2^{-1}$$

where

$h_1(t)$, $h_2(t)$, $h_3(t)$ are the components of $\underline{H}_N(t)$,

$d_1(t)$, $d_2(t)$, $d_3(t)$ are the components of $\underline{d}_B(t)$.

or, in more compact notation,

$$\frac{d}{dt}\underline{x} = F\underline{x} + G(t)\,\underline{d}_B(t) + \tau_{dist,B} \tag{14}$$

APPLICATION OF THE LINEAR QUADRATIC REGULATOR (LQR)

Since it is desirable to maintain R, P, and Y as close to zero as possible over time, a reasonable cost function is the standard quadratic performance index [6]. We wish to minimize

$$J(\underline{d}_B(t)) = \lim_{t_f \to \infty} \frac{1}{2} \underline{x}^T(t_f) \, S_f \, \underline{x}(t_f) + \frac{1}{2} \int_{t_0}^{t_f} \left[\underline{x}^T(t) \, A \, \underline{x}(t) + \underline{d}^T_B(t) \, B \, \underline{d}_B(t) \right] dt \tag{15}$$

subject to the state equation

$$\underline{\dot{x}}(t) = F \, \underline{x}(t) + G(t) \, \underline{d}_B(t) \ ,$$

where A is positive definite and B is non-negative-definite, assuming that $\tau_{dist,B} = 0$ in equation (14). This problem has a well-known solution given by

$$\underline{d}_B(t) = -B^{-1} G^T(t) \, S(t) \, \underline{x}(t) \ , \tag{16}$$

where the square matrix S(t) satisfies the Riccati differential equation

$$\dot{S}(t) = -S(t)F - F^T S(t) + S(t)G(t)B^{-1}G^T(t)S(t) - A \tag{17}$$

with the terminal condition $S(t_f) = S_f$. This equation can be integrated backward in time to give the time-varying feedback gain matrix $K(t) \equiv -B^{-1}G^T(t)S(t)$. The dependence of S(t) on S_f becomes negligible as t_f becomes large, a fact which can be exploited to give K(t) as if we were actually solving the problem with $t_f \to \infty$. That is, t_f is chosen far enough ahead that its effect is not seen at the present, and S_f, which can be any appropriately dimensioned non-negative-definite symmetric matrix, is set to zero.

Kalman [8] has shown for a time-varying linear system, that if controllability is uniform over time, the closed loop infinite-time-horizon LQR is exponentially stable.

RESULTS OF NUMERICAL SIMULATIONS

The algorithm outlined above was simulated on an AT-class personal computer. The Riccati equation was solved numericallly using a fourth-order Runge-Kutta integrator, with time scaling to keep the system numerically well conditioned. The geomagnetic field was modelled using an 8th-order spherical harmonic expansion, as described in Wertz [9]. Nonlinear equations for rigid body dynamics and gravity gradient torques were used in the plant model. The feedback control law, while derived for the linearized plant equations, was applied to this nonlinear plant. The orbit used was near-circular and near-polar.

Cost function matrices A and B were chosen empirically to produce desirable performance. Attention, however, was restricted to matrices of the form

$$A = \begin{bmatrix} a_\theta & & & & & \\ & a_\theta & & & & \\ & & a_\theta & & & \\ & & & a_\omega & & \\ & & & & a_\omega & \\ & & & & & a_\omega \end{bmatrix}, \text{ and } B = \begin{bmatrix} b & & \\ & b & \\ & & b \end{bmatrix}$$

where a_θ, a_ω, $b > 0$.

In all cases tested, the closed loop system was stable. A simple check of controller sensitivity was made by using a slightly different model for the closed loop simulation than was assumed in computing the feedback gain. Moments of inertia, orbit eccentricity, and perigee position were varied, and in each case the system remained stable, though performance was degraded slightly, as expected.

The satellite mass properties, orbit, and disturbance parameters used in evaluations are given in Table 1. The disturbance torques used are based on a 2 m² area and a 30 cm center of pressure to center of mass offset. This is conservative for a satellite with a maximum moment of inertia of 27 kg-m². Figures 2A through 2E show time histories of Euler angles for several configurations.

APPLICATION OF GEOMETRIC PROPERTIES

Direct implementation of the time-varying linear-feedback control law described above requires a numerical solution of the matrix Riccati differential equation. Since the equation is solved backward from a future time to compute feedback gains at the present time, the integration must be restarted repetitively, each starting at a point later in time, as illustrated in Figure 3.

Obviously, integration backward in time is not ideal for real-time implementation. Fortunately, however, we can utilize the quasi-periodicity due to orbit geometry to advantage, making real-time implementation feasible.

We wish to parameterize the feedback gain $K(t)$ in terms of position rather than time. First, we make certain assumptions about the orbit:

(1) Orbit has a known semi-major axis, a
(2) Orbit is circular, $e = 0$
(3) Orbit has known inclination, i
(4) Node is inertially fixed, $d\Omega/dt = 0$
(5) Perigee is inertially fixed, $d\omega/dt = 0$
(6) Orbital angular rate is known, ω_o
(7) Earth rotational rate is known, ω_E

These assumptions will typically be valid over several days, which is adequate for our purposes. Referring to Figure 4, it becomes simple to describe an entire satellite trajectory, $\underline{r}(t)$, in Earth fixed coordinates, in terms of only $\beta(t_o)$ and $\lambda(t_o)$ at any fixed time t_o:

$$\underline{r}(t) = R_3\big(\omega_E(t-t_o) - \lambda(t_o)\big) R_1(-i) R_3\big(-\beta(t_o) - \omega_o(t-t_o)\big) \begin{bmatrix} 1 \\ 0 \\ 0 \end{bmatrix} \qquad (18)$$

The insight to be gained here is that if the trajectory can be completely parameterized in terms of the ordered pair $(\beta(t_o),\lambda(t_o))$ then the geomagnetic field history, $\underline{H}_N(t)$ can be similarly expressed in terms of (β,λ). Hence the feedback gain matrix $K(t_o)$, which depends on $\underline{H}_N(t)$ from $t_o<t<\infty$, can be written as a function of $(\beta(t_o),\lambda(t_o))$ only. This function, $K(\beta,\lambda)$, is not time varying. Thus, $K(\beta,\lambda)$ can be computed once and will remain valid permanently.

A real orbit will not satisfy the assumptions exactly. We can, however, drop the assumption of a circular orbit; the expression in equation (18) then becomes much more tedious, but the conclusion is the same. That is, the trajectory can be completely characterized by (β,λ).

When assumptions (4) and (5) are violated by a small amount, the effect is to add a slow time variation to $K(\beta,\lambda)$. In an implementation of this system, $K(\beta,\lambda)$ must be recomputed periodically. It is expected that recomputing once every three days will be adequate for a typical perigee drift rate of three degrees/day. This requires much less CPU time than the continuous gain computation of Figure 3.

The feedback gain function $K(\beta,\lambda)$ has been computed for several cases. It appears to be reasonably well behaved and can be represented with a modest investment in computer memory. Interestingly, a secondary advantage of using (β,λ) to parameterize $K(\cdot)$, rather than another position representation scheme, is that $K(\beta,\lambda)$ is periodic in both β and λ with a period of 2π. It may be possible to reduce data storage requirements by representing $K(\beta,\lambda)$ in terms of Fourier coefficients.

FLIGHT SOFTWARE CONFIGURATION

A suggested flight software configuration is given in Figure 5. The infrequent updating of the feedback gains is run as a background task, and the Real Time Control operation is the high priority task.

Since both tasks require a model of the orbit, periodic orbit updates from a ground station will be necessary. It is believed that updates on the order of once every seven days should be adequate for most applications.

CONCLUSIONS

The feasibility of spacecraft attitude control using only magnetic torquing has been demonstrated. Although the closed-loop transient reaction speed possible with such a system is fundamentally limited, the attitude requirements of many missions appear attainable. An algorithm for flight computer implementation has been simulated, demonstrating the feasibility of using this system with a typical onboard microprocessor. The mechanical simplicity inherent in using electromagnetics only for control promises to make such a system both cost effective and mechanically reliable.

REFERENCES

[1] Junkins, J. L., C. K. Carrington, and C. E. Williams, "Time Optimal Magnetic Attitude Maneuvers," presented at AIAA/AAS Astrodynamics Conference, Danvers, Massachusetts, August 1980.

[2] Glaese, J. R., et al, "Low-Cost Space Telescope Pointing Control System," *Journal of Spacecraft and Rockets*, Volume 13, No. 7, pp. 400-405, July 1976.

[3] Carlucci, D., et al, "Attitude Estimation and Satellite Detumbling by Active Magnetic Controls," *Journal of Control and Computers*, Volume 12, No. 3, pp. 100-103, 1984.

[4] Schmidt, G. E., Jr., "The Application of Magnetic Attitude Control to a Momentum Biased Synchronous Communications Satellite," presented at AIAA Guidance and Control Conference, Boston, Massachusetts, August 1975.

[5] Bruderle, E., and A. Reindler, "Magnetic Roll/Yaw Attitude Control of a Momentum Biased Near Polar Orbit Satellite," IFAC Automatic Control in Space 1982, Proceedings of the Ninth Symposium, Noordwijkerhout, Netherlands, July 1982.

[6] Elbert, T. F., Estimation and Control of Systems, Van Nostrand Reinhold Company, New York, pp. 304-319, 1984.

[7] Martel, F., P. K. Pal, and M. Psiaki, "Active Magnetic Control System for Gravity Gradient Stabilized Spacecraft," Proceedings of the Second Annual AIAA/USU Conference on Small Satellites, September 1988.

[8] Kalman, R. E., "Contributions to the Theory of Optimal Control," *Bol. Soc. Mat. Mexicana*, pp. 102-119, 1960.

[9] Wertz, J. R., ed., Spacecraft Attitude Determination and Control, D. Reidel Publishing Company, Boston, Massachusetts, pp. 117-123, 1985.

32

Table 1

System Parameters Used in Test Cases of Table 2

Moments of Inertia

	I_1	27	kg-m^2
	I_2	27	kg-m^2
	I_3	10	kg-m$_2$

Orbital Rate

	ω_o	1.0473E-3	rad/s

Orbit

Semi-major axis	a	1.15537	earth radii
Eccentricity	e	0.004119	
Inclination	i	89.547	degrees
Right ascension of the ascending node	Ω_N	111.167	degrees
Arg. of perigee	ω_P	71.0035	degrees
Node drift rate	$d\Omega_N/dt$	-0.047522	deg/day
Per. drift rate	$d\omega_P/dt$	-3.004395	deg/day
Epoch day		130	
Time of day		78194.5	sec
Year		87	

Orbservation Time Span

Simulations start at 1987, day 131, time = 100 sec.

Disturbances Used in Performance Analysis

Torque (constant in body frame)

±55	dyne-cm	in Roll
±100	dyne-cm	in Pitch
±10	dyne-cm	in Yaw

Residual Magnetic Dipole (constant in body frame)

200	pole-cm	in body x-axis
200	pole-cm	in body y-axis
200	pole-cm	in body z-axis
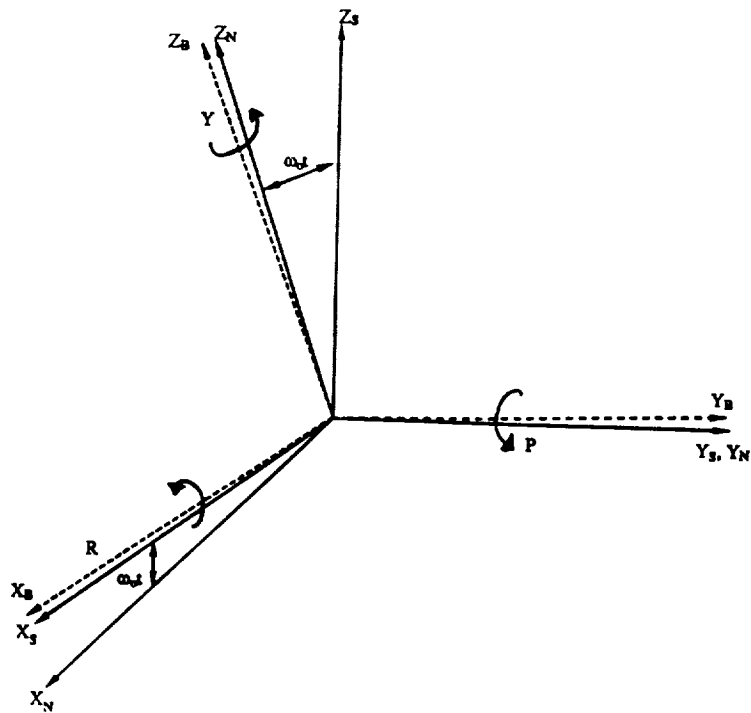
$X_S = Y_S \times Z_S$
Y_S = orbit normal
Z_S = center of earth to S/C position at time t=0

$X_N = Y_N \times Z_N$
Y_N = orbit normal
Z_N = local vertical (up)

P = Pitch
Y = Yaw

Figure 1: Coordinate System and Small 2-1-3 Euler Angle Definitions
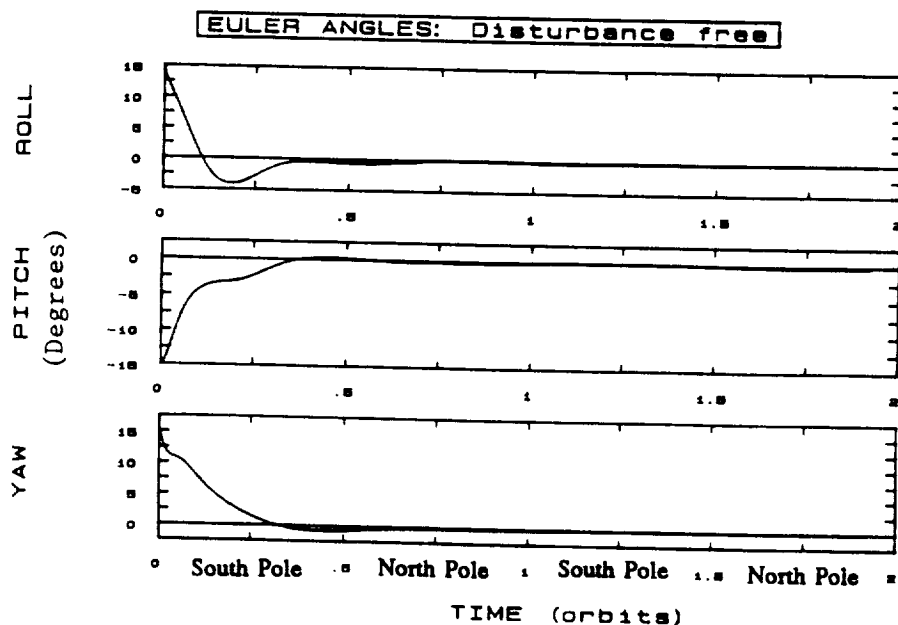
Figure 2a: Time history of Euler angles for a case without any disturbance torques or a residual dipole. Note that angles do not decay precisely to zero because the orbit is not perfectly circular.

34
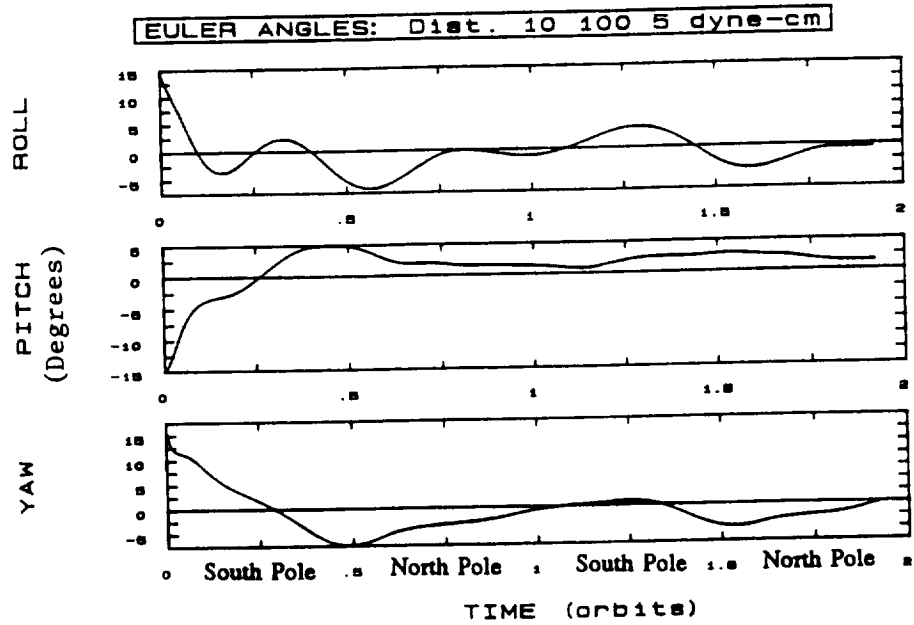
Figure 2b: Case where disturbance torque is a constant +10 dyne-cm in roll, +100 dyne-cm in pitch, and +5 dyne-cm in yaw. A residual dipole of 200 i + 200 j + 200 k pole-cm is also assumed.
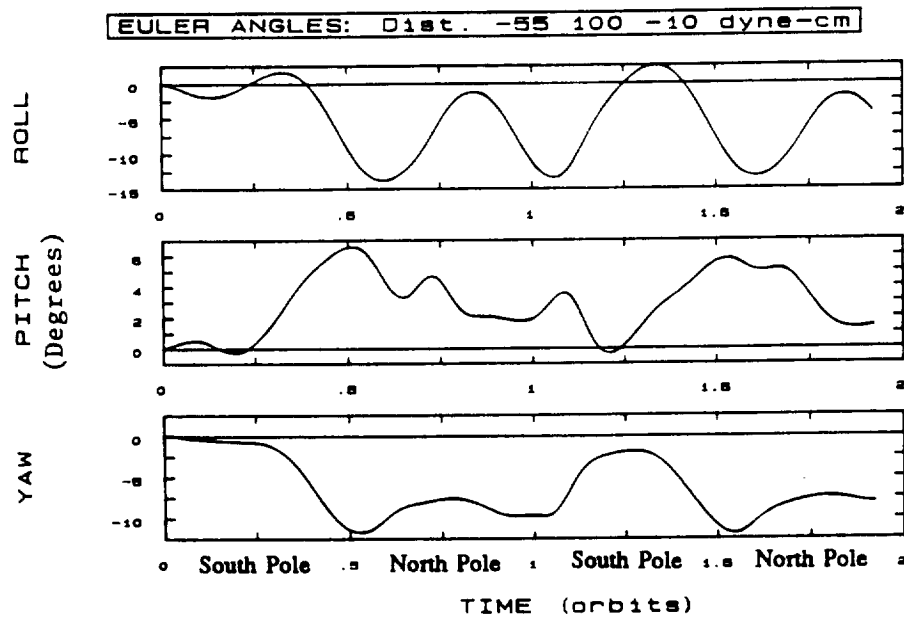
Figure 2c: Disturbance torque for this case is a constant -55 dyne-cm in roll, +100 dyne-cm in pitch, and -10 dyne-cm in yaw. A residual dipole of 200 i + 200 j + 200 k pole-cm is also assumed.

EULER ANGLES: Dist. 55 100 10 dyne-cm

ROLL

PITCH (Degrees)

YAW

o   South Pole   .5   North Pole   1   South Pole   1.5   North Pole   2

TIME (orbits)
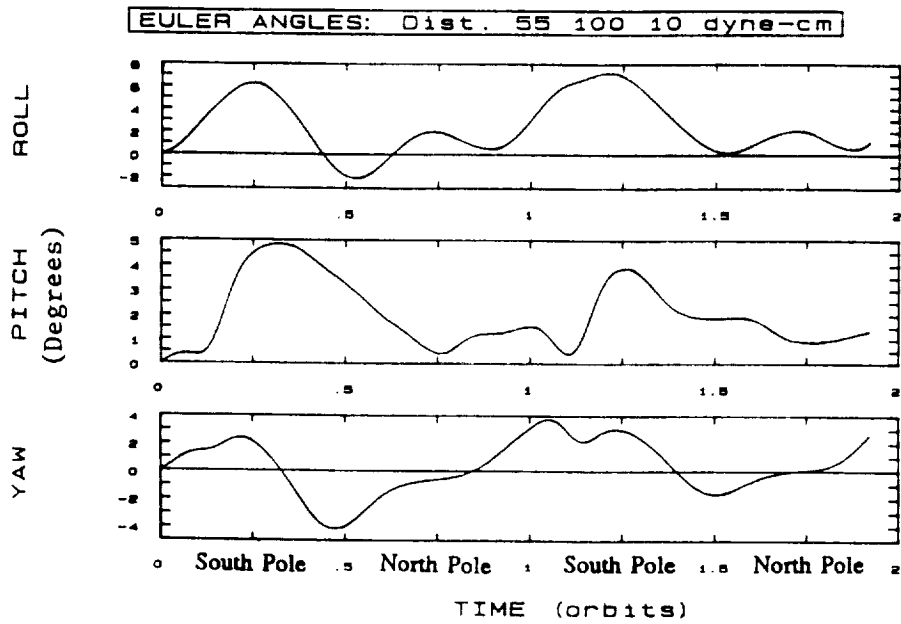
Figure 2d: The disturbance torque assumed for this case is +55 dyne-cm in roll, +100 dyne-cm in pitch, and +10 dyne-cm in yaw. A residual dipole of 200 i + 200 j + 200 k pole-cm is also assumed.

EULER ANGLES: Dist. -55 100 -10 dyne-cm

ROLL

PITCH (Degrees)

YAW

o   South Pole   .5   North Pole   1   South Pole   1.5   North Pole   2

TIME (orbits)
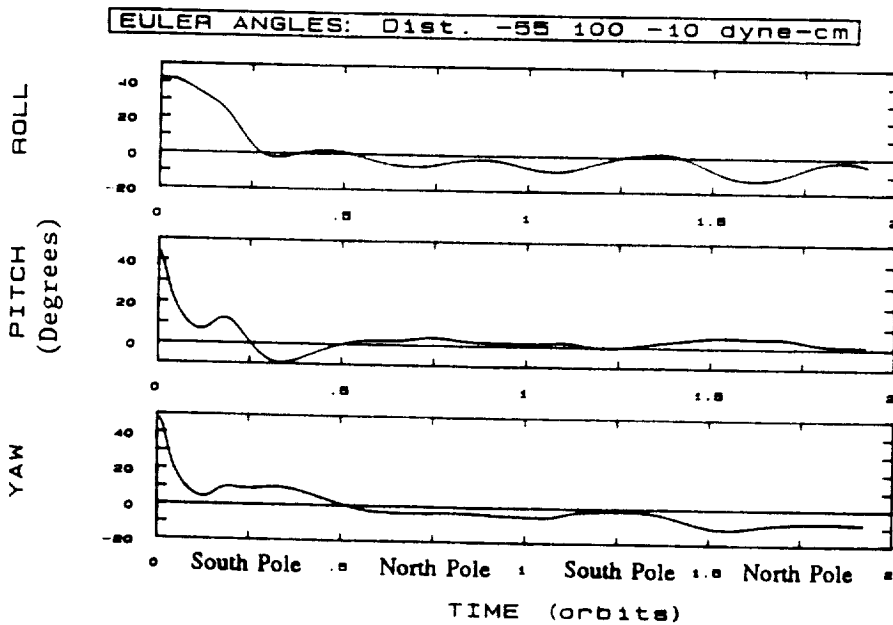
Figure 2e: Disturbance torque is a constant -55 dyne-cm in roll, +100 dyne-cm in pitch, and -10 dyne-cm in yaw. A residual dipole of 200 i + 200 j + 200 k pole-cm is also assumed. The closed loop system will not capture reliably at initial angles larger than 40°.

36
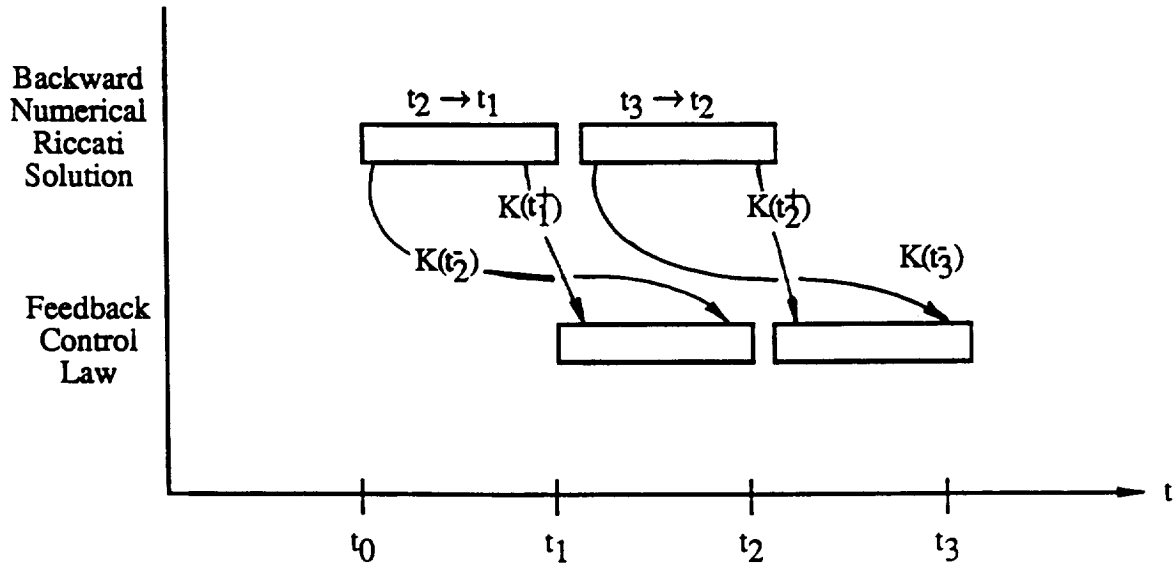
Figure 3: Iteration necessary when using backward Riccati equation integration in real time.
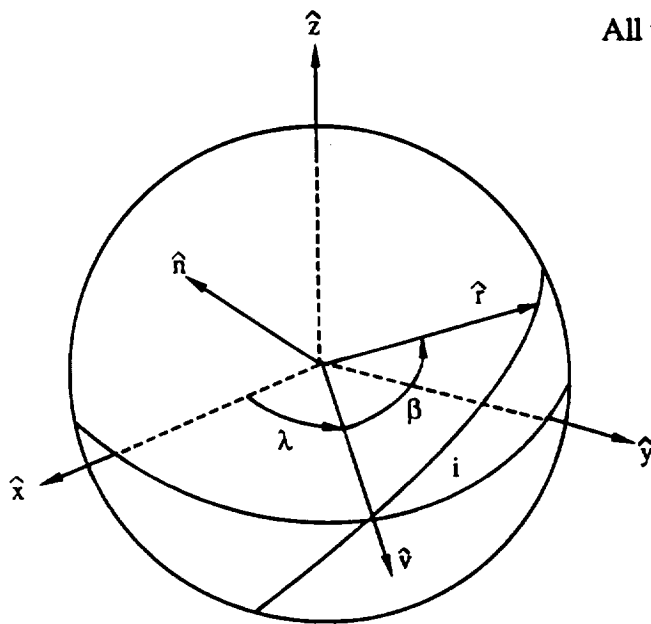
All vectors represented in Earth-fixed coordinates.

$\hat{n}$ = positive orbit normal

$\hat{r}$ = direction to spacecraft

$$\hat{v} = \frac{\hat{z} \times \hat{n}}{\left| \hat{z} \times \hat{n} \right|} = \text{direction of ascending node}$$

$$\beta = \tan^{-1}_{(2 \text{ arg})} \left\{ \frac{\hat{r} \cdot (\hat{n} \times \hat{v})}{\hat{r} \cdot \hat{v}} \right\}$$

$$\lambda = \tan^{-1}_{(2 \text{ arg})} \left\{ \frac{\hat{v} \cdot \hat{y}}{\hat{v} \cdot \hat{x}} \right\}$$

$\hat{x}, \hat{y}, \hat{z}$ Earth-fixed coordinate axes, with $\hat{z}$ = north

Notes:

(1) $\frac{d\lambda}{dt} \approx -\omega_E$, $\omega_E = 2\pi$ radians/24 hours

(2) For near circular orbit, $\frac{d\beta}{dt} \approx \omega_o$, ω_o = orbital angular rate (rad/sec)

Figure 4: Definition of position parameters β and λ.
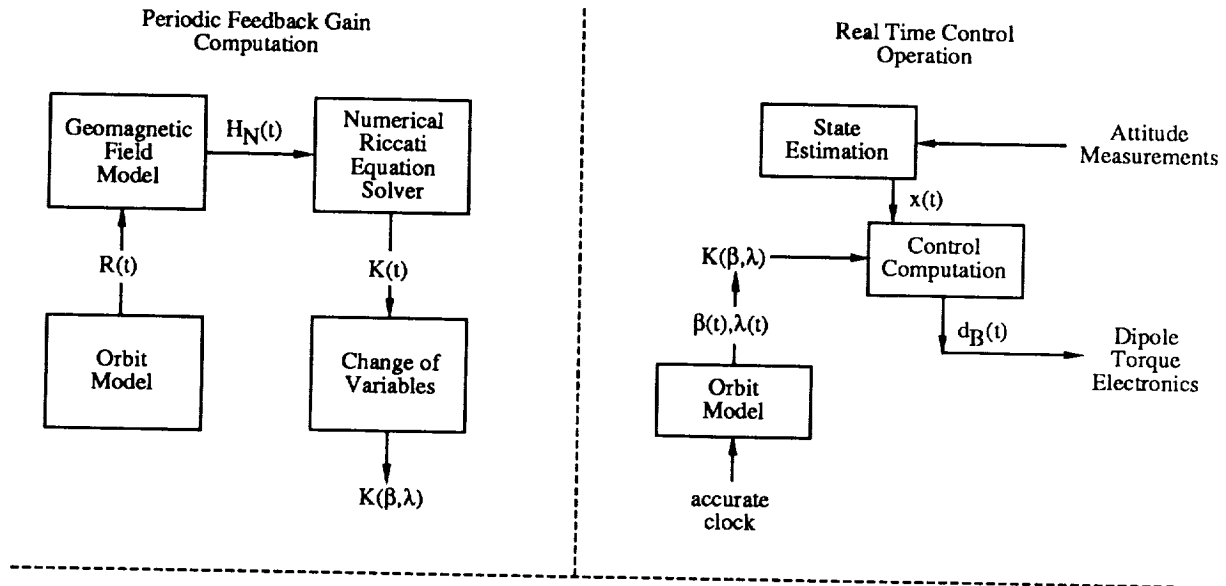
Figure 5: Control Software Structure